

# Nanoscale

Accepted Manuscript



This is an *Accepted Manuscript*, which has been through the Royal Society of Chemistry peer review process and has been accepted for publication.

*Accepted Manuscripts* are published online shortly after acceptance, before technical editing, formatting and proof reading. Using this free service, authors can make their results available to the community, in citable form, before we publish the edited article. We will replace this *Accepted Manuscript* with the edited and formatted *Advance Article* as soon as it is available.

You can find more information about *Accepted Manuscripts* in the [Information for Authors](#).

Please note that technical editing may introduce minor changes to the text and/or graphics, which may alter content. The journal's standard [Terms & Conditions](#) and the [Ethical guidelines](#) still apply. In no event shall the Royal Society of Chemistry be held responsible for any errors or omissions in this *Accepted Manuscript* or any consequences arising from the use of any information it contains.

## pH-programmable self-assembly of plasmonic nanoparticles: hydrophobic interaction *verse* electrostatic repulsion

Weikun Li, Istvan Kanyo, Chung-Hao Kuo, Srinivas Thanneeru, Jie He\*

Department of Chemistry, University of Connecticut, Storrs, CT 06269

Email: jie.he@uconn.edu

### Abstract

We report a general strategy to conceptualize a new design for pH-programmable self-assembly of plasmonic gold nanoparticles (AuNPs) tethered by random copolymers of poly(styrene-*co*-acrylic acid) (P(St-*co*-AA)). It is based on using pH as an external stimulus to reversibly change the surface charge of polymer tethers and to control the delicate balance of interparticle attractive and repulsive interactions. By incorporating -COOH moieties locally within PSt hydrophobic segments, the change in ionization degree of -COOH moieties can dramatically disrupt the hydrophobic attraction within a close distance. pH acts as a key parameter to control the deprotonation of -COOH moieties and “programs” the assembled nanostructures of plasmonic nanoparticles in a stepwise manner. At a higher solution pH where -COOH groups of polymer tethers became highly deprotonated, the electrostatic repulsion dominated the self-assembly and it favored the formation of the end-to-end, anisotropic assemblies, *e.g.* 1-D single-line chains. At a lower pH, the less deprotonated -COOH groups led to the decrease of electrostatic repulsion and the side-to-side aggregates, *e.g.* clusters and multi-line chains of AuNPs, became favorable. The pH-programmable self-assembly allowed us to engineer a “manual” program for a sequential self-assembly by changing pH of the solution. We demonstrated that the two-step pH-programmable assembly could generate more sophisticated “multi-block” chains using two different sized AuNPs. Our strategy offers a general means for the programmable design of plasmonic nanoparticles into the specific pre-ordained nanostructures that is potentially useful for the precise control over their plasmon coupling.

## 1. Introduction

The recent integration of metal nanoparticles (NPs) with amphiphilic polymer tethers has emerged conceptually as a new class of building blocks for self-assembly, namely amphiphilic colloidal molecules (ACMs).<sup>1-12</sup> Driven by the amphiphilicity of polymer tethers, ACMs can spontaneously assemble into a variety of nanostructures. Such self-assembly determines the interparticle distance of metal cores, and rules the plasmon coupling of metal NPs that is of great interest for numerous applications, *e.g.* sensors,<sup>13-15</sup> photovoltaic devices,<sup>16, 17</sup> bioimaging,<sup>18, 19</sup> and cancer therapy.<sup>20-22</sup> Engineering the surface ligands of ACMs (*e.g.* chemical compositions, density and distribution) is a facile, efficient way to control the site-specific interactions between neighboring metal NPs and/or the surrounding medium,<sup>23-30</sup> thus resulting in their self-organization in a controlled/directed manner. However, compared to pure amphiphilic molecules (*e.g.* polymers and surfactants), the significant increase of interparticle or intermolecular forces (*e.g.* van der Waals force and hydrophobic interactions) due to the size of building blocks has largely increased the complexity of ACM self-assembly.<sup>1, 31-34</sup> Moreover, the slow “dynamic” effect of ACMs can easily trap a variety of intermediate assemblies with sophisticated structures, beyond the capability of amphiphilic molecules. As such, the challenges to design and program the assembly nanostructures of ACMs are noticeable. Despite tremendous progress in controlling the self-assembly of ACMs,<sup>1, 35-39</sup> so far the rational design of programmable self-assembly of ACMs into the specific pre-ordained nanostructures is still lacking.

Herein we present a general strategy to conceptualize a new design for the programmable self-assembly of ACMs. It is based on using pH as an external stimulus to reversibly change the surface charge of polymer tethers and to control the delicate balance of interparticle interactions, *i.e.* the attractive and repulsive forces. This method allows us to program the assembly intermediates of ACMs in a stepwise manner by changing the solution pH. As a proof-of-concept, we designed ACMs consisting of gold NPs (AuNPs) tethered by amphiphilic random copolymers of poly(styrene-*co*-acrylic acid) (P(St-*co*-AA)). Differing from the latest examples of self-assembly of ACMs driven by the amphiphilicity of block copolymer and mixed polymer brushes,<sup>4, 8, 9</sup> the use of random copolymers of P(St-*co*-AA) has the perceived merits of, i) a predesigned length and functionality of polymer tethers and chemical composition (*i.e.* the ratio of hydrophilic/hydrophobic units), and ii) a precise control over interparticle interaction of ACMs that enables the controllability of assembly intermediates. The insertion of ionizable moieties in hydrophobic PSt tethers can dramatically disrupt the hydrophobic force within a close distance. We demonstrated that the spatial self-organization of ACMs could be controlled by tuning the electrostatic forces between neighboring NPs under different pHs.<sup>1</sup> The pH-programmable self-assembly of charged ACMs also offers a great controllability to generate more sophisticated nanostructures, *e.g.* multi-block chains. Our approach stands out as a straightforward and powerful method to manipulate the assemblies of ACMs

and it may illustrate a new pathway for programmable self-assembly of plasmonic nanoparticles with tunable collective properties.<sup>40</sup>

## 2. Experimental Section

### 2.1 Materials

Hydrogen tetrachloroaurate trihydrate ( $\text{HAuCl}_4 \cdot 3\text{H}_2\text{O}$ , >99.9%), cetyltrimethylammonium bromide (CTAB, 99%), ascorbic acid, sodium borohydride ( $\text{NaBH}_4$ , >99%), trisodium citrate, and trifluoroacetic acid (99%) were purchased from Sigma-Aldrich and used without further purification unless otherwise noted. *tert*-Butyl acrylate (98%) and styrene (99%) were passed through a basic aluminum oxide column prior to use. Azobisisobutyronitrile (AIBN) was recrystallized twice from ethanol. The RAFT chain transfer agent (CTA), 2-(2-cyanopropyl) dithiobenzoate (CPDB), was prepared according to a previously reported method.<sup>41</sup> Deionized water (High-Q, Inc. 103S Stills) with resistivity of >10.0 M $\Omega$  was used in all experiments. The pH values of the solution were adjusted by adding either a standard 1.0 M of KOH solution or 1.0 M of HCl solution, both calibrated by a pH meter.

### 2.2 Polymer synthesis and characterizations

#### *Synthesis of poly(styrene-co-*tert*-butyl acrylate)(P(St-co-*t*BA)) using RAFT polymerization*

The random copolymer of poly(styrene-co-*tert*-butyl acrylate) (P(St-co-*t*BA)) was synthesized via the one-step RAFT polymerization procedure as reported. To prepare P(St-co-*t*BA), styrene (41.6 g, 0.4 mol), *tert*-butyl acrylate (15.4 g, 0.12 mol), CPDB (221 mg, 1.0 mmol) and AIBN (30 mg, 0.183 mmol) were first dissolved in 20 mL of anisole (99%, anhydride) in a 100 mL flask. The mixture was then degassed under vacuum for 10 min and refilled with nitrogen three times. Next, the flask was placed in a pre-heated oil bath at 80°C for 15 h. After cooling the solution mixture to room temperature, the polymer was precipitated in cold ethanol three times and dried under vacuum at 40°C for 24 h. From GPC measurements using polystyrene standards, the polymer sample has a  $M_n(\text{GPC})$  of 31.0 Kg/mol and a polydispersity index (PDI,  $M_w/M_n$ ) = 1.20. From the <sup>1</sup>H NMR spectrum (in  $\text{CDCl}_3$ ), the NMR-based  $M_n(\text{NMR})$  is 28.3 kg/mol, using the integrals of the resonance peaks of aromatic ring in CPDB (7.4-7.9 ppm).

#### *Synthesis of thiol-ended Poly(styrene-co-*tert*-butyl acrylate) (P(St-co-*t*BA)-SH)*

To obtain the thiol-functionalized random copolymer, the dithioester ended P(St-co-*t*BA) random copolymer was reduced by *n*-butylamine in THF. P(St<sub>188</sub>-co-*t*BA<sub>68</sub>) (10 g, 0.2 mmol) and *n*-butylamine (0.8 g, 11 mmol) were dissolved in THF. The reaction was carried out under nitrogen for 2 h until the color of solution changed from light red to yellow. The polymer was then precipitated in a water/ethanol mixture (1/3, vol) twice and dried under vacuum for 24 h.

#### *Synthesis of thiol-ended poly(styrene-co-acrylic acid) (P(St<sub>188</sub>-co-(*t*BA<sub>1-x</sub>-co-AA<sub>x</sub>)<sub>68</sub>-SH)*

Thiol-ended P(St<sub>188-co-tBA</sub><sub>68</sub>) (35.0 g) was dissolved in deuterated chloroform (40 mL) in a 100 mL flask, followed by the addition of trifluoroacetic acid (11.4 g) (1 equiv with respect to the *tert*-butyl ester groups). The reaction was monitored by <sup>1</sup>H NMR. Two samples were taken at 1 h and 3 h. Subsequently, 11.4 g of trifluoroacetic acid was added into the reaction mixture and two samples were taken after another 1 h and 3 h. Next, 11.4 g of trifluoroacetic acid was added. Two more samples were obtained at 3 h and 24 h. To purify the polymers, trifluoroacetic acid was removed by use of a rotary evaporator. The obtained polymer was dissolved in dichloromethane and precipitated in ethanol twice. The polymer was then dried overnight at 40 °C under vacuum. The hydrolysis degree of *tert*-butyl groups was calculated from <sup>1</sup>H NMR spectra (see supporting information for details).

### 2.3 Synthesis, surface modification and self-assembly of AuNPs

#### *Synthesis of AuNPs*

The synthetic details of AuNPs are given in the supporting information.

#### *Surface modification of AuNPs*

AuNPs with a core diameter of 8.5 nm were modified using a biphasic ligand-exchange approach. Typically, 4 mL of chloroform was added to approximately 40 mL of aqueous solution (~0.037 mg mL<sup>-1</sup>) of AuNPs which standing for 1 h in order to sufficiently extract excess CTAB in the aqueous solution. After the organic phase was removed, the resulting aqueous solution (100 mL) was added to 100 mL of PSt<sub>188-co-P</sub>(tBA<sub>0.42-co-AA</sub><sub>0.58</sub>)<sub>68</sub> (20 mg, 0.6 μmol) in THF/CHCl<sub>3</sub> (9:1), followed by sonication for 1 h and incubation for 24 h. The final solution separated into two layers and the red lower layer of AuNP solution (in CHCl<sub>3</sub> phase) was obtained. The solution of AuNPs was further concentrated and then precipitated twice in ethanol. Then, random copolymer modified AuNPs were further purified by centrifugation 10-12 times and redispersed in DMF at a concentration of 0.15 mg/mL.

AuNPs with a diameter of 15 and 29 nm were modified using direct ligand-exchange in DMF. Typically, 10 mg of thiol-ended PSt<sub>188-co-P</sub>(tBA<sub>0.42-co-AA</sub><sub>0.58</sub>)<sub>68</sub> was first dissolved in 10 mL of DMF. Then, a concentrated solution of AuNPs (~2 mg/mL) was slowly added to the above solution under sonication and then incubated overnight. The modified AuNPs were purified by centrifugation 5-6 times and redispersed in DMF at a concentration of 0.05 mg/L.

#### *Self-assembly of ACMs in the DMF/water solution*

The self-assembly of ACMs was triggered by the slow addition of water as a selective solvent. Briefly, 0.5 mL of water/DMF solution with an initial water concentration ( $C_w$ ) of 30 vol% was slowly added to 0.5 mL of ACM solution (0.05 mg/mL in DMF). The final concentration of water was  $C_w=15$  vol% for the self-assembly. The mixed solution was slowly shaken for 2 hr, and then a drop of solution (2-5 μL) was cast on a carbon coated copper grid for TEM observation. The different pHs of self-assembly solution were adjusted by a standard 1.0 M of KOH solution or 1.0 M of HCl solution. *Note that*, the pH values used in this study are the pHs of the initial water.

## 2.4 Characterizations

GPC measurements were performed on a Waters GPC-1 (1515 HPLC Pump and Waters 717Plus Autoinjector) equipped with a Varian 380-LC evaporative light scattering detector and a Waters 2487 dual absorbance detector, three Jordi Gel fluorinated DVB columns (1-100K, 2-10K and 1-500Å). THF was used as an elution solvent at a flow rate of 2.0 mL/min and PSt standards were used for molecular weight and molecular weight distribution calibration. The data was processed using Empower™ GPC software (Waters, Inc.). Proton nuclear magnetic resonance (<sup>1</sup>H NMR) spectra were recorded on a Bruker Avance 300 MHz spectrometer. High-resolution transmission electron microscopy (HR-TEM) studies were carried out using a JEOL 2010 transmission electron microscope with an accelerating voltage of 200 kV. The TEM samples were prepared by casting the suspension of assemblies on a carbon coated copper grid (300 mesh). The Raman spectra were recorded on Renishaw System 2000 equipped with four lasers (488nm, 514nm, 633nm, 785nm). Raman scattering intensity was collected with the accumulation time of 30 s for 3 integrals. For each sample, three independent measurements were performed to average the Raman intensity. ζ-potential measurements were characterized using a ZetaPlus (Brookhaven Instruments, Holtsville, NY) with a SR-516 type electrode. The ζ-potential of NPs was measured in DMF. Three runs were averaged for each sample and ζ-potentials were calculated using Smoluchowski fits to the data with software. The UV-vis spectra of AuNPs before and after self-assembly were recorded on a Cary 60 UV-Vis spectrophotometer: The assemblies in DMF/water were placed in quartz sample cell with a cell path length of 5 mm.

## 3. Results and Discussion

Amphiphilic random copolymers tethered ACMs were designed and prepared according to reported procedures.<sup>5,9</sup>  
<sup>42</sup> The amphiphilic random copolymer of poly(styrene-*co-tert*-butyl acrylate) (PSt<sub>188-co-PtBA</sub><sub>68</sub>,  $M_n=28.6$  kg/mol, PDI=1.18) with thiol terminal groups was first synthesized using reversible addition fragmentation chain transfer (RAFT) polymerization, followed by the reduction of dithioester to thiol using *n*-butyl amine (see SI for synthetic details). Subsequently, the deprotection of *tert*-butyl groups was carried out in the presence of trifluoroacetic acid. By varying the hydrolysis reaction time, seven polymers with different PAA contents were obtained, denoted as PSt<sub>188-co-P(tBA<sub>1-x-co-AA</sub>)<sub>68</sub> where  $x$  indicates the hydrolysis degree of *tert*-butyl groups ( $x=0, 0.03, 0.19, 0.39, 0.58, 0.69, \text{ and } 1.00$ ) (see Table 1 and Fig S1). Using the ligand exchange reaction in dimethylformamide (DMF), the thiol-terminated amphiphilic copolymers of PSt<sub>188-co-P(tBA<sub>1-x-co-AA</sub>)<sub>68</sub> were grafted onto AuNPs via covalent Au-S bonds. The polymer-grafted AuNPs were purified by at least 5 centrifugation cycles in DMF to remove free polymer. As estimated from the polymer corona thickness in high-magnification TEM images,<sup>5,9</sup> the average grafting density of polymers is 0.1~0.3 nm<sup>-2</sup> for 15-nm AuNPs depending on the hydrolysis degree (Fig S2). The tethered ACMs are denoted as AuNP- $D$ - $PN$  hereafter, where  $D$  is the average diameter of AuNPs and  $N$  is the sample number of polymers as given in Table 1. The random copolymer modified AuNPs exhibited</sub></sub>

amphiphilic behavior by stabilizing the Pickering emulsion of toluene-in-water (Fig S4). The amphiphilic ACMs preferably remained at the toluene/water interface to minimize interfacial energy. It is interesting to note that, the Pickering emulsion is pH-responsive (AuNP-15-P5). By adding NaOH solution to change the pH of the aqueous phase to  $\sim 10$ , the toluene-in-water emulsion was disrupted and two phases appeared. The emulsion could be readily re-formed by changing pH back to 7 using HCl solution. This implies that, the ionization degree of carboxylic acid groups of polymer tethers can reversibly switch the hydrophobicity of ACMs, thus leading to the pH-sensitive emulsion.

**Table 1.** Characterizations of amphiphilic random copolymers

Samples	Polymer compositions <sup>a</sup>	Hydrolysis degree of <i>t</i> BA <sup>a</sup>	Percentage of AA units ( $\phi_{AA}$ ) <sup>b</sup>
P1	PSt <sub>188</sub> - <i>co</i> -P <i>t</i> BA <sub>68</sub>	0	0
P2	PSt <sub>188</sub> - <i>co</i> -P( <i>t</i> BA <sub>0.97</sub> - <i>co</i> -AA <sub>0.03</sub> ) <sub>68</sub>	0.03	0.8%
P3	PSt <sub>188</sub> - <i>co</i> -P( <i>t</i> BA <sub>0.81</sub> - <i>co</i> -AA <sub>0.19</sub> ) <sub>68</sub>	0.19	5.1%
P4	PSt <sub>188</sub> - <i>co</i> -P( <i>t</i> BA <sub>0.61</sub> - <i>co</i> -AA <sub>0.39</sub> ) <sub>68</sub>	0.39	10.3%
P5	PSt <sub>188</sub> - <i>co</i> -P( <i>t</i> BA <sub>0.42</sub> - <i>co</i> -AA <sub>0.58</sub> ) <sub>68</sub>	0.58	15.4%
P6	PSt <sub>188</sub> - <i>co</i> -P( <i>t</i> BA <sub>0.31</sub> - <i>co</i> -AA <sub>0.69</sub> ) <sub>68</sub>	0.69	18.3%
P7	PSt <sub>188</sub> - <i>co</i> -PAA <sub>68</sub>	1.00	26.6%

Note: <sup>a</sup> the polymer compositions and hydrolysis degree of *t*BA groups were directly measured from <sup>1</sup>H NMR; <sup>b</sup> the percentage of AA units was the mole fraction of AA units in polymer chains.

We first studied the amphiphilicity-driven self-assembly of ACMs tethered by random copolymers of PSt<sub>188</sub>-*co*-P(*t*BA<sub>1-x</sub>-*co*-AA<sub>x</sub>)<sub>68</sub>. Using AuNP-15-P5 as an example, the self-assembly was triggered by adding a selective solvent, water, to its DMF solution. The overall water concentration for all samples was  $\sim 15$  vol%, at which the hydrophobic PSt segments became insoluble and the solubility of P*t*BA and PAA segments was unaltered. To minimize the overall free energy, the PSt segments collapsed, resulting in the self-assembly of ACMs. Under natural conditions, after adding water to the DMF solution of AuNP-15-P5, the end-to-end single-line chain was formed with an interparticle distance of  $10.5 \pm 2.6$  nm (Fig 1c). By adjusting the pH of water using HCl or NaOH solution, the self-assembly and dissociation can be programmed by pH. For example, when decreasing the pH of solution from 5 (Fig 1b) to 4 (Fig 1a), the ACMs of AuNP-15-P5 could form clusters and multi-line chains of AuNPs, respectively.<sup>42, 43</sup> On the contrary, by changing pH to 9 using NaOH solution, the assemblies of AuNPs were completely disrupted and unimolecular micelles were found to be well-dispersed in DMF/water solution. The morphological transition of AuNP-15-P5 was also accompanied by a colorimetric response of AuNPs, as a result of the change in plasmon coupling of neighboring AuNPs (Fig 1e). The decrease of pH obviously induced the color change from red, to purple, and eventually to blue. The corresponded extinction spectra are given in Fig 1f. Compared with individual AuNPs, the surface plasmon resonance peak of one dimensional (1-D) chains had a large red-shift from 530 to 625 nm, which possibly arose from the 1-D transverse plasmon coupling between AuNPs along chains.<sup>44</sup> It further confirms the morphological transition of assemblies in solution at different pHs.<sup>45</sup>

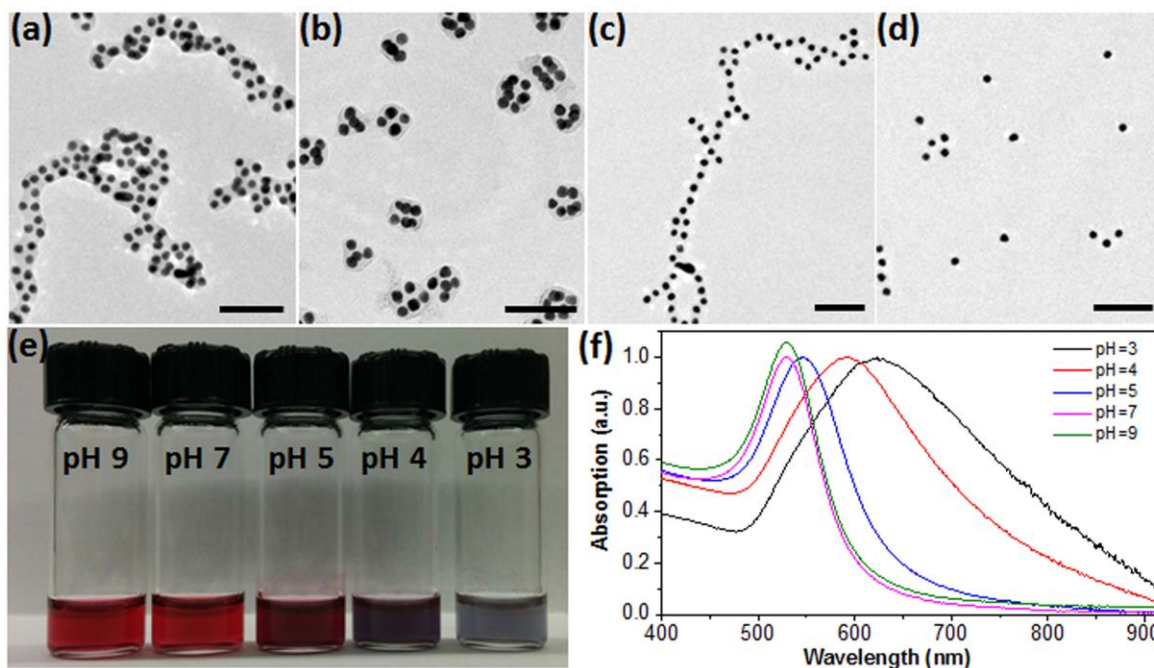


**Figure 1.** pH-programmable self-assembly of AuNP-15-P5. (a-d) TEM images of ACM assemblies obtained at different pHs in water/DMF (15/85, vol) solution: (a) multi-line chains at pH=4.0; (b) clusters at pH=5.0; (c) single-line chains at pH=7.0; and (d) unimolecular micelles at pH=9.0. The self-assembly time of all samples is 2 hr. Scale bars are 100 nm in (a-d). (e) Digital picture of the self-assembly of AuNP-15-P5 in response to the changes of pH. (f) The extinction spectra of assembled AuNP-15-P5 in the pH range of 3-9 at room temperature.

The self-assembly of charged AuNPs embodies a delicate interplay and balance of various attractive and repulsive interactions exerted on AuNPs, *e.g.* hydrophobic attraction, van der Waals attraction and electrostatic repulsion.<sup>42, 46-49</sup> The attractive force favors more contact between polymer tethers and drives the formations of more compact, side-to-side aggregates of AuNPs (*e.g.* clusters). Unlike the hydrophobic attraction, the electrostatic repulsive force is largely dependent on the distribution of electric ACM double layers. The electrostatic repulsive force acts as a key driving force to form anisotropic self-assemblies (*e.g.* end-to-end 1-D chains) immediately after the formation of initial dimers in order to minimize the electrostatic repulsion.<sup>48</sup> As recently reported by Choueiri *et al.*,<sup>42</sup> the total potential energy change of such system is  $\Delta E = \Delta E_a + \Delta E_r$ , where  $\Delta E_a$  is the contribution of attractive forces and  $\Delta E_r$  is the contribution term of repulsive forces. The attraction term, known as the hydrophobic interaction of polymer tethers, can be calculated from the change in interfacial tension between the polymer ligands and solvents. It is essentially constant if the length of hydrophobic PSt segment is fixed. The repulsion term of  $\Delta E_r$  for two charged ACMs can be expressed as  $\Delta E_r = \frac{\psi^2}{4\pi\epsilon_0\epsilon(1+L_e d)} \frac{\exp[-L_e(l-d)]}{l}$ , where  $\psi$  is the surface potential of NPs,  $\epsilon_0$  and  $\epsilon$  are the dielectric constants of vacuum and solution,  $d$  is the diameter of NPs,  $l$  is the center-to-center distance of two neighboring NPs, and  $L_e$  is the Debye length, respectively.<sup>50, 51</sup> The surface charge density becomes critical in determining the repulsive contribution to the change of overall potential energy; that is,

a slight increase of surface charge of ACMs can significantly increase the repulsion potential of two neighboring NPs. Under basic conditions (pH~9), the highly deprotonated -COOH groups could locally enhance the repulsive term that shifts the balance of attractive and repulsive interactions, and discrete ACMs would be obtained (Fig 1d). The decrease of solution pH reduced the ionization degree of -COOH groups. When the attractive interactions started to balance out the repulsive interactions, the formation of 1-D chains was observed (Fig 1c). A further decrease in solution pH would result in attractive interactions playing a more crucial role. Clusters of AuNPs, and eventually the multi-line chains containing both end-to-end and side-to-side organized AuNPs were formed. In this case, the more compact aggregates become favorable. For such a pH-programmable self-assembly of ACMs, the robustness of utilizing random copolymers lies in the precise control over the balance of hydrophobic attraction and electrostatic repulsion which surpasses the capability of block copolymers and mixed polymer brushes.

The surface charge of ACMs can also be controlled by the content of surface -COOH groups, thus enabling another possible pathway to tune the electrostatic repulsive interaction and manipulate the assembled nanostructures of ACMs. By controlling the hydrolysis of *tert*-butyl groups, the percentage of -COOH groups ( $\phi_{AA}$ ) in polymer tethers can be varied from 0% to 26.6%. Figure 2 shows the nanochains obtained from 15 nm AuNPs tethered with P1 ( $\phi_{AA}=0\%$ ), P2 ( $\phi_{AA}=0.8\%$ ) and P3 ( $\phi_{AA}=5.1\%$ ) at pH=7. AuNP-15-P1 formed multi-line chains when no -COOH groups were present on the surface of AuNPs (Fig 2a). The multi-line chains have an average diameter of ~28 nm, containing 2~3 side-by-side AuNPs in the transverse direction. The length of multi-line chains is quite polydisperse, in the range of hundreds of nanometers to several micrometers. With a further increase of the -COOH groups of polymer tethers, morphological transitions occurred, to mixed chains (Fig 2b,  $\phi_{AA}=0.8\%$ ), and single-line chains (Fig 2c,  $\phi_{AA}=5.1\%$ ). The single-line chains were obtained until  $\phi_{AA}=18.3\%$  and discrete NPs were observed at  $\phi_{AA}=26.6\%$ . This, again, suggests the tunability of electrostatic repulsion by the density of surface -COOH groups. This was further confirmed by  $\zeta$ -potential of ACMs. With the increase of -COOH groups from 0% to 26.6%, the  $\zeta$ -potential of ACMs increased from ~0 to -60 mV (Fig S5). The end-to-end self-assembly was favorable when the repulsive force dominated.

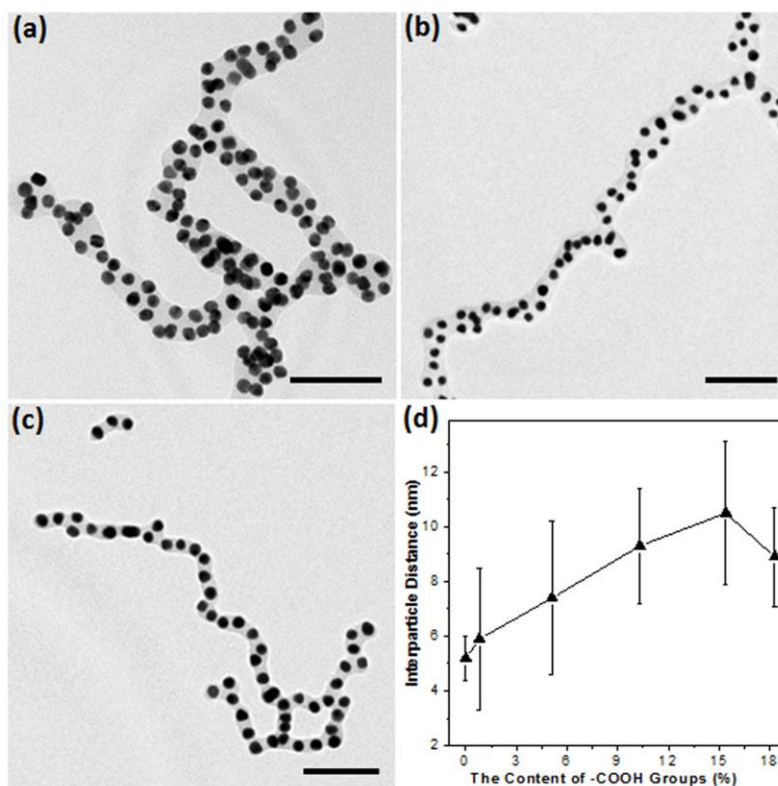


**Figure 2.** (a-c) TEM images of 1-D chains by adjusting the content of -COOH groups ( $\varphi_{AA}$ ) in polymer tethers of ACMs: (a)  $\varphi_{AA} = 0\%$ ; (b)  $\varphi_{AA} = 0.8\%$ , and (c)  $\varphi_{AA} = 5.1\%$ . All assemblies were obtained at pH=7 with 15 vol% of water. The self-assembly time is 2 hr. Scale bars are 100 nm in (a-c). (d) Plot of interparticle distance as a function of the content of -COOH groups. All the data were measured by averaging at least 100 particles from TEM images. Error bars represent the standard deviation. The interparticle distance in multi-line chains was calculated from the diameter of chains and average size of AuNPs.

Assuming that the mean-square end-to-end distance of polymer tethers ( $R_0$ ) was not significantly changed by the hydrolysis, the interparticle distance of AuNPs is largely depended on the repulsive interaction of adjacent NPs. As shown in Fig 2d, the average interparticle distance gradually increased from  $5.2 \pm 0.8$  nm to  $10.5 \pm 2.6$  nm with a gradual increase of  $\varphi_{AA}$  from 0% to 15.4% (Fig S3 for details). This result is also highly consistent with the pH-dependence of interparticle distance, indicating an increase in surface charge density. The increase of interparticle electrostatic repulsion with a higher -COOH content would result in the increase of interparticle distances. We note that the interparticle distance of the AuNPs slightly decreased to  $8.9 \pm 1.8$  nm at  $\varphi_{AA} = 18.3\%$  which might be due to the between solubility of polymer at a higher -COOH content. The change in interparticle distance affected the plasmon coupling between AuNPs, further confirmed by surface-enhanced Raman scattering results (see Fig S15).<sup>52</sup>

To gain more insight into the self-assembly behavior of charged ACMs, the morphological transitions were systematically investigated by varying the contents of -COOH groups and pHs (Fig 3). The boundaries of a phase-

like diagram clearly suggest that, when fewer -COOH groups were present in the polymers and at a lower assembly solution pH, multi-line chains containing side-to-side aggregates were favorable; while, higher pHs and more -COOH content result in end-to-end aggregates and unimolecular micelles. The morphologies of ACMs are dependent on both pH and the content of -COOH groups. For instance, at a fixed pH =9 of the solution, the transitions from multi-line chains to single-line chains, and to unimolecular micelles of the  $\phi_{AA}$  occur from 0% to 26.6% (see Fig S7). Likewise, similar morphological transitions can be observed by decreasing solution pH from 9 to 3 (see Fig S9-13). Of particular note, without -COOH groups in polymer tethers (*e.g.* AuNP-15-P1), the self-assembly showed no dependence on pH at all (Fig S8).

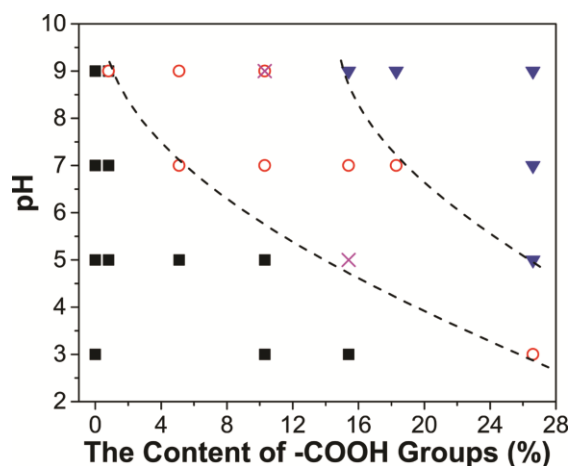


**Figure 3.** Phase-like diagram of the self-assembly of ACMs with different  $\phi_{AA}$  and pHs: multi-line chains (■); single-line chains (○); unimolecular micelles (▼) and clusters (×). *Note that*, two symbols were plotted at one data point, indicating that two primary aggregates co-existing under the same experimental conditions.

The self-assembly morphologies can possibly be influenced by the size of Au cores as the size determines the absolute number of polymer tethers on an individual ACM. When decreasing the size of Au cores to 8 nm, all ACMs of AuNP-8 assembled into multi-line chain nanostructures, even at a higher  $\phi_{AA}$  of 15.4% (Fig S16). This is essentially because of lower surface charge on smaller ACMs and less repulsion forces of neighboring NPs (Fig S6).<sup>47, 49</sup> For ACMs of AuNP-29, by varying the polymer tethers, morphological transitions were observed from multi-line chains (Fig 4a, AuNP-29-P1) to single-line chains (Fig 4b, AuNP-29-P3), then to unimolecular micelles (Fig 4c, AuNP-29-P5), similar to AuNP-15. When varying the solution pH from 3 to 9 for AuNP-29-P3, we also observed the morphological multi-line chains (pH=3) (Fig 4d) and unimolecular micelles (pH=9) (Fig 4e). These results imply that the step-wise programmable assembly of ACMs is universal for different sizes of ACMs. At the same time, we also observed the morphological transitions in THF/H<sub>2</sub>O solution (Fig S18).

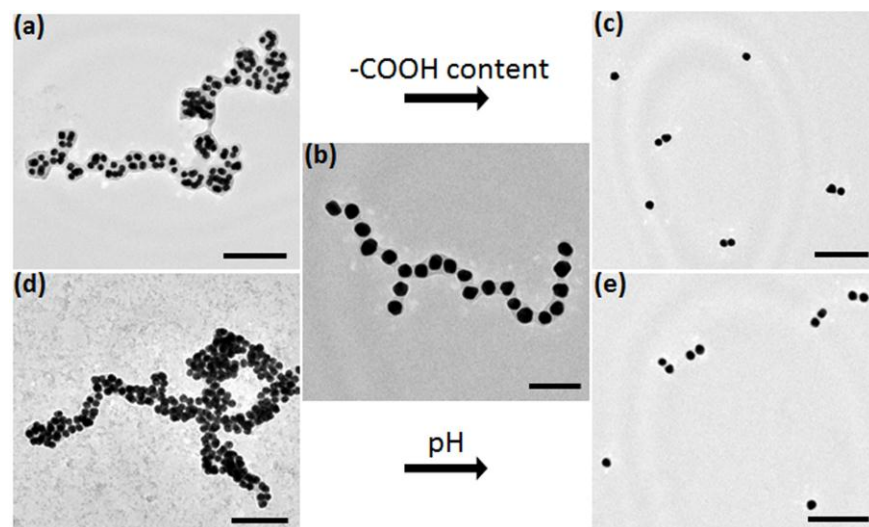


**Figure 4.** The assembled nanostructures of ACMs of AuNP-29 by varying  $\phi_{AA}$  and pHs in water/DMF. (a-c) TEM images of multi-line chains or clusters (a, AuNP-29-P1), single-line chains (b, AuNP-29-P3) and unimolecular micelles (c, AuNP-29-P5) obtained using different polymer tethers at pH=7. (d, b, e) TEM images of the morphological transitions of AuNP-29-P3 from multi-line chains (d, pH=3), single-line chains (b, pH=7) to single particles (e, pH=9) by varying pHs. Scale bars are 200 nm in (a, c-e) and 100 nm in (b).

To confirm that self-assembly occurred in solution, using AuNP-29-P3 as an example, we further studied the self-assembly kinetics of chains by dynamic light scattering (DLS) (Fig S19). In pure DMF, the average hydrodynamic diameter ( $D_h$ ) of AuNP-29-P3 is  $\sim 58$  nm, close to the core-shell size of AuNPs and polymer tethers. Note that, the mean-square end-to-end distance ( $R_0$ ) of P3 is approximately 11 nm, calculated from  $R_0 = bN^{0.5}$ , where  $b$  is the Kuhn monomer length, with  $b = 1.8$  nm for PSt block, and  $N$  is the ‘degree of polymerization’ obtained from the molar mass of the Kuhn monomer  $M_0$  ( $M_0 = 720$  g mol $^{-1}$  for PSt).<sup>53</sup> It indicates that ACMs of AuNP-29-P3 were well-dispersed in DMF. By slowly adding water to reach the concentration of  $\sim 15$  vol%, the  $D_h$  of AuNP-29-P3 gradually increased and reached  $\sim 117$  nm after 5 min. This is likely because of the formation of ACM dimers or trimers at the beginning. When increasing the self-assembly time, two distinct peaks are observed at 80 nm and 500 nm; while, the intensity of peak at  $D_h \sim 500$  nm increased and the intensity of peak at  $D_h \sim 80$  nm decreased in the course of self-assembly, suggesting the appearance of chain structures. By further increasing the self-assembly time to 100 min, a new peak of  $D_h \sim 1400$  nm presented. The increase in the larger hydrodynamic size of aggregates is ascribed to the formation of long and branched nanochains in solution,<sup>54</sup> consistent with our TEM observation.

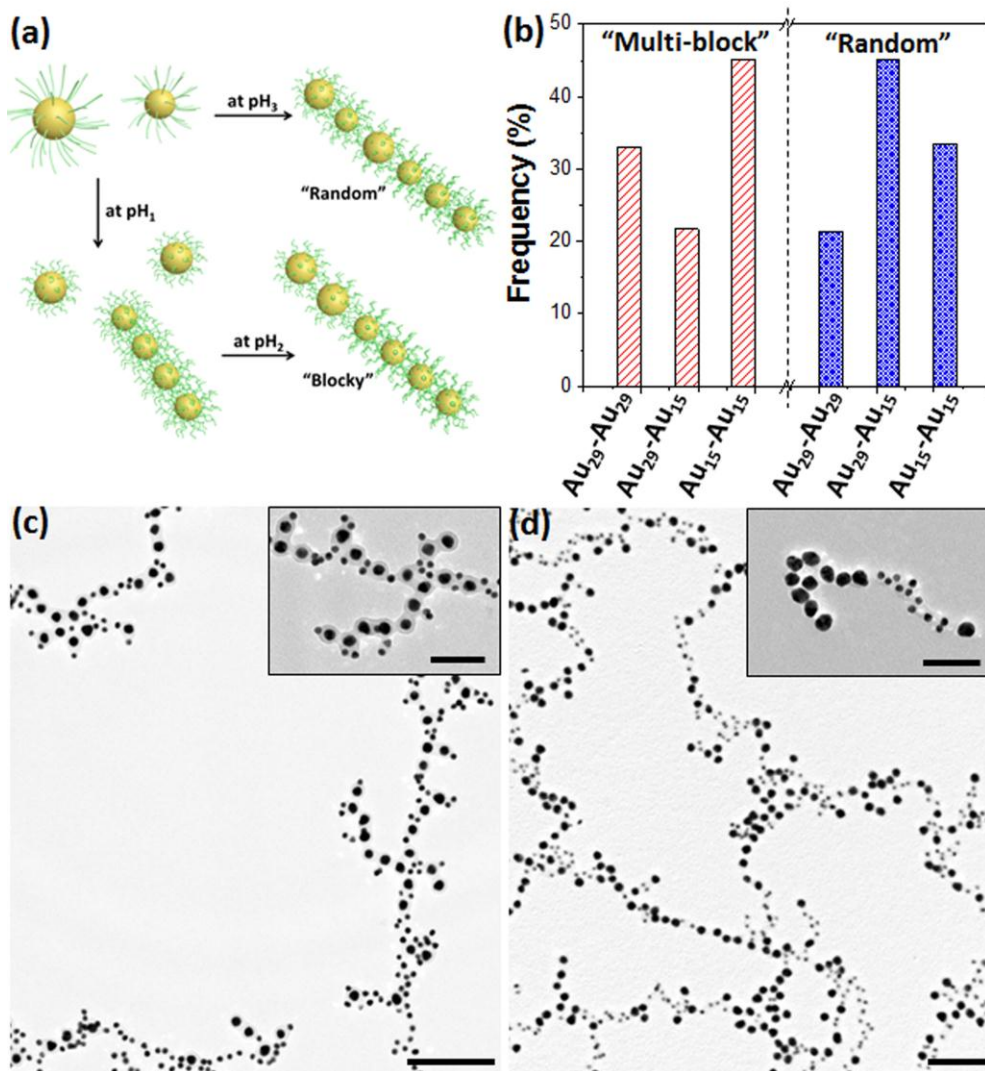


**Figure 5.** (a) Schematic illustration of the formation of “multi-block” chain and random chain from two-sized ACMs using pH-programmable self-assembly. (b) Statistic distribution of the resulting linear composite ACMs chains with different coupling configurations of AuNP-15-P1 and AuNP-29-P3. The frequency was averaged from >500 particles. (c,d) Low magnification TEM images of random chain (c) obtained by single-step assembly and “multi-block” chain (d) obtained by two-step programmable assembly using two-sized ACMs of AuNP-15-P1 and AuNP-29-P3. Scale bars are 200 nm in (c,d) and 100 nm in insets of (c,d).

The pH-programmable self-assembly of charged ACMs offers a major advancement to generate more sophisticated nanostructures. Inspired by the polymerization techniques of random copolymers and block copolymers, we have investigated a “manual” program for the self-assembly sequence of ACMs where they can be built “bottom up” from two ACMs,<sup>55</sup> when co-assembling two types of ACMs that consist of different pH-responsive random polymer tethers.<sup>43, 56</sup> As illustrated in Fig 5a, the co-assembly of two different ACMs normally results in the formation of “random” chains, similar to the random copolymerization of two arbitrary monomers. However, if the competition of such assembly kinetics can be remotely activated or controlled by solution pH, the

growth of chains can be programmed in a sequentially “blocky” manner. For instance, at  $\text{pH}_1$ , the larger ACMs were first deactivated to assemble and the self-assembly only occurs between smaller ACMs; afterwards, by changing the pH to  $\text{pH}_2$  to activate the larger ACMs, the “blocky” sequence of ACMs should be obtained (Fig 5a).

As a proof-of-concept, we have investigated the co-assembly of AuNP-15-P1 (irresponsive to the change of pH) and AuNP-29-P3. The individual solutions of AuNP-15-P1 and AuNP-29-P3 in DMF were first mixed at a number ratio of NPs,  $\sim 1:1$ . The addition of water, at natural conditions, would trigger the random co-assembly of AuNP-15-P1 and AuNP-29-P3 (Fig 5c). The histogram of statistical distribution of coupling conformation in the linear chains as denoted,  $\text{Au}_{29}\text{-Au}_{29}$ ,  $\text{Au}_{29}\text{-Au}_{15}$ , and  $\text{Au}_{15}\text{-Au}_{15}$ , is plotted in Fig 5b. The frequency of  $\text{Au}_{29}\text{-Au}_{15}$  conformation is  $\sim 45.1\%$ , suggesting a random distribution of AuNP-15-P1 and AuNP-29-P3 in the chains. Alternatively, the two-step programmable assembly was carried out by a constitutive pH change at  $\text{pH}\sim 9$  and  $\text{pH}\sim 5$ . At a water concentration of 10 vol% and  $\text{pH}\sim 9$ , the ACMs of AuNP-15-P1 first assembled into multi-line chains, while the ACMs of AuNP-29-P3 were “deactivated” for self-assembly under the above conditions. By further decreasing solution pH to 5 (the final water content  $\sim 20$  wt%), the AuNP-29-P3 started to assemble and form single-line chains at the end of AuNP-15-P1 multi-line chains (Fig 5d). As a result,  $\text{Au}_{29}\text{-Au}_{29}$  and  $\text{Au}_{15}\text{-Au}_{15}$  became the main population of coupling conformation with a frequency of 33.1% and 45.2% (Fig 5b), respectively, indicating the formation of a larger fraction of blocky nanostructures.

#### 4. Conclusions

In summary, we have demonstrated the pH-programmable self-assembly of ACMs tethered by amphiphilic random polymers in selective solvents. By incorporating -COOH groups locally within PSt hydrophobic segments, the pH-controllable long-range electrostatic repulsions can effectively tune the self-assembly of polymer-tethered plasmonic NPs. Such ACMs could self-assemble to unimolecular micelles, single-line chains, clusters, or multi-line chains in the mixed solvent of water/DMF, depending on the solution pH, the content of -COOH groups in polymer tethers, and the size of Au cores. By utilizing the pH-responsiveness of polymer tethers, we further exploited two-step programmable assembly to generate more sophisticated “multi-block” chains and random chains from two-sized ACMs. Our studies could open up a new realm of programmable self-assembly of charged ACMs that are potentially useful for functional materials and devices.

#### Acknowledgments

JH thanks the financial support of startup funds from the University of Connecticut. We thank Prof. Vijay Kumar for the DLS and  $\zeta$ -potential measurements and Dr. Lichun Zhang for technical assistance on TEM imaging. This work was partially supported by the Green Emulsions Micelles and Surfactants (GEMS) Center.

### Supporting Information

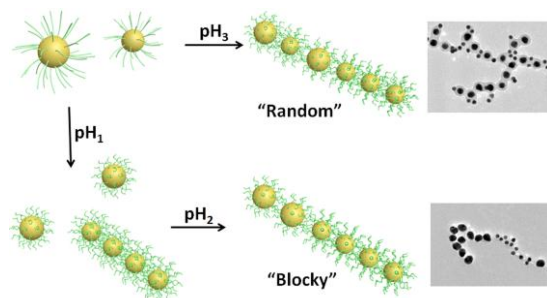
The synthesis and characterizations of polymers, NPs and ACMs, more low-magnification TEM images, the reversible self-assembly results and the effect of core sizes and solvents on self-assemblies of ACMs. This material is available free of charge via the Internet.

## References

1. M. Grzelczak and L. M. Liz-Marzán, *J. Phys. Chem. Lett.*, 2014, **5**, 2455-2463.
2. M. G. Moffitt, *J. Phys. Chem. Lett.*, 2013, **4**, 3654-3666.
3. A. Klinkova, R. M. Choueiri and E. Kumacheva, *Chem. Soc. Rev.*, 2014, **43**, 3976-3991.
4. E. R. Zubarev, J. Xu, A. Sayyad and J. D. Gibson, *J. Am. Chem. Soc.*, 2006, **128**, 15098-15099.
5. Z. H. Nie, D. Fava, E. Kumacheva, S. Zou, G. C. Walker and M. Rubinstein, *Nat. Mater.*, 2007, **6**, 609-614.
6. K. Liu, Z. Nie, N. Zhao, W. Li, M. Rubinstein and E. Kumacheva, *Science*, 2010, **329**, 197-200.
7. Y. Mai and A. Eisenberg, *J. Am. Chem. Soc.*, 2010, **132**, 10078-10084.
8. J. Song, L. Cheng, A. Liu, J. Yin, M. Kuang and H. Duan, *J. Am. Chem. Soc.*, 2011, **133**, 10760-10763.
9. J. He, Y. Liu, T. Babu, Z. Wei and Z. Nie, *J. Am. Chem. Soc.*, 2012, **134**, 11342-11345.
10. J. He, X. Huang, Y.-C. Li, Y. Liu, T. Babu, M. A. Aronova, S. Wang, Z. Lu, X. Chen and Z. Nie, *J. Am. Chem. Soc.*, 2013, **135**, 7974-7984.
11. Y. J. Liu, Y. C. Li, J. He, K. J. Duelle, Z. Y. Lu and Z. H. Nie, *J. Am. Chem. Soc.*, 2014, **136**, 2602-2610.
12. M. Grzelczak, A. Sanchez-Iglesias, H. H. Mezerji, S. Bals, J. Perez-Juste and L. M. Liz-Marzan, *Nano Lett*, 2012, **12**, 4380-4384.
13. J. N. Anker, W. P. Hall, O. Lyandres, N. C. Shah, J. Zhao and R. P. Van Duyne, *Nat. Mater.*, 2008, **7**, 442-453.
14. M. Grzelczak and L. M. Liz-Marzán, *Langmuir*, 2013, **29**, 4652-4663.
15. G. Chen, Y. Wang, M. Yang, J. Xu, S. J. Goh, M. Pan and H. Chen, *J. Am. Chem. Soc.*, 2010, **132**, 3644-3645.
16. D. M. Guldi, I. Zilbermann, G. Anderson, N. A. Kotov, N. Tagmatarchis and M. Prato, *J. Mater. Chem.*, 2005, **15**, 114.
17. Z. Nie, A. Petukhova and E. Kumacheva, *Nat. Nanotechnol.*, 2010, **5**, 15-25.
18. M. J. Sailor and J. H. Park, *Adv. Mater.*, 2012, **24**, 3779-3802.
19. J. Song, J. Zhou and H. Duan, *J. Am. Chem. Soc.*, 2012, **134**, 13458-13469.
20. J. He, Z. Wei, L. Wang, Z. Tomova, T. Babu, C. Wang, X. Han, J. T. Fourkas and Z. Nie, *Angew. Chem. Int. Ed.*, 2013, **52**, 2463-2468.
21. J. Song, Z. Fang, C. Wang, J. Zhou, B. Duan, L. Pu and H. Duan, *Nanoscale*, 2013, **5**, 5816-5824.
22. Z. Yin, W. Zhang, Q. Fu, H. Yue, W. Wei, P. Tang, W. Li, W. Li, L. Lin, G. Ma and D. Ma, *Small*, 2014, **10**, 3619-3624.
23. S. C. Glotzer and M. J. Solomon, *Nat. Mater.*, 2007, **6**, 557-562.
24. G. A. Devries, M. Brunnbauer, Y. Hu, A. M. Jackson, B. Long, B. T. Neltner, O. Uzun, B. H. Wunsch and F. Stellacci, *Science*, 2007, **315**, 358-361.
25. Y. Wang, Y. Wang, D. R. Breed, V. N. Manoharan, L. Feng, A. D. Hollingsworth, M. Weck and D. J. Pine, *Nature*, 2012, **491**, 51-55.
26. Z. L. Zhang, M. A. Horsch, M. H. Lamm and S. C. Glotzer, *Nano Lett.*, 2003, **3**, 1341-1346.
27. W.-B. Zhang, X. Yu, C.-L. Wang, H.-J. Sun, I. F. Hsieh, Y. Li, X.-H. Dong, K. Yue, R. Van Horn and S. Z. D. Cheng, *Macromolecules*, 2014, **47**, 1221-1239.
28. Y. Liu, X. Han, L. He and Y. Yin, *Angew. Chem. Int. Ed.*, 2012, **51**, 6373-6377.
29. H.-Y. Lee, S. H. R. Shin, A. M. Drews, A. M. Chirsan, S. A. Lewis and K. J. M. Bishop, *ACS Nano*, 2014, **8**, 9979-9987.
30. W. Li, C.-H. Kuo, I. Kanyo, S. Thanneeru and J. He, *Macromolecules*, 2014, **47**, 5932-5941.
31. Y. Liu, X.-M. Lin, Y. Sun and T. Rajh, *J. Am. Chem. Soc.*, 2013, **135**, 3764-3767.
32. Y. Min, M. Akbulut, K. Kristiansen, Y. Golan and J. Israelachvili, *Nat. Mater.*, 2008, **7**, 527-538.
33. A. Sanchez-Iglesias, M. Grzelczak, T. Altantzis, B. Goris, J. Perez-Juste, S. Bals, G. Van Tendeloo, S. H. Donaldson, Jr., B. F. Chmelka, J. N. Israelachvili and L. M. Liz-Marzan, *ACS Nano*, 2012, **6**, 11059-11065.
34. H. Zhang, Y. Liu, D. Yao and B. Yang, *Chem. Soc. Rev.*, 2012, **41**, 6066-6088.
35. J. Pyun, *Polym. Rev.*, 2007, **47**, 231-263.
36. K. K. Zhang, M. Jiang and D. Y. Chen, *Prog. Polym. Sci.*, 2012, **37**, 445-486.

37. M. Grzelczak, J. Vermant, E. M. Furst and L. M. Liz-Marzan, *ACS Nano*, 2010, **4**, 3591-3605.
38. Y.-F. Cheng, X.-D. Lai, Y. Yan, J.-Y. Peng, X. Yu, C. Ye, C.-L. Fu, J.-Y. Liu, Y.-X. Chen and J.-Q. Hu, *RSC Adv*, 2013, **3**, 19942-19945.
39. X. Feng, F. Ruan, R. Hong, J. Ye, J. Hu, G. Hu and Z. Yang, *Langmuir*, 2011, **27**, 2204-2210.
40. K. J. M. Bishop, C. E. Wilmer, S. Soh and B. A. Grzybowski, *Small*, 2009, **5**, 1600-1630.
41. J. S. Song and M. A. Winnik, *Macromolecules*, 2006, **39**, 8318-8325.
42. R. M. Choueiri, A. Klinkova, H. Therien-Aubin, M. Rubinstein and E. Kumacheva, *J. Am. Chem. Soc.*, 2013, **135**, 10262-10265.
43. H. Wang, L. Chen, X. Shen, L. Zhu, J. He and H. Chen, *Angew. Chem. Int. Ed.*, 2012, **51**, 8021-8025.
44. K. Liu, A. Lukach, K. Sugikawa, S. Chung, J. Vickery, H. Therien-Aubin, B. Yang, M. Rubinstein and E. Kumacheva, *Angew. Chem. Int. Ed.*, 2014, **53**, 2648-2653.
45. Z. Sun, W. Ni, Z. Yang, X. Kou, L. Li and J. Wang, *Small*, 2008, **4**, 1287-1292.
46. Z. Tang and N. A. Kotov, *Adv. Mater.*, 2005, **17**, 951-962.
47. M. Yang, G. Chen, Y. Zhao, G. Silber, Y. Wang, S. Xing, Y. Han and H. Chen, *PCCP*, 2010, **12**, 11850-11860.
48. H. Zhang, K.-H. Fung, J. Hartmann, C. T. Chan and D. Wang, *J. Phys. Chem. C*, 2008, **112**, 16830-16839.
49. H. Zhang and D. Wang, *Angew. Chem. Int. Ed.*, 2008, **120**, 4048-4051.
50. K. J. Bishop, C. E. Wilmer, S. Soh and B. A. Grzybowski, *Small*, 2009, **5**, 1600-1630.
51. J. N. Israelachvili, *Intermolecular and surface forces*, Burlington, 3rd edn., 2011.
52. M. Yang, T. Chen, W. S. Lau, Y. Wang, Q. Tang, Y. Yang and H. Chen, *Small*, 2009, **5**, 198-202.
53. M. Rubinstein and R. H. Colby, *Polymer physics*, Oxford University Press, Oxford ; New York, 2003.
54. S. Lin, M. Li, E. Dujardin, C. Girard and S. Mann, *Adv. Mater.*, 2005, **17**, 2553-2559.
55. H. Wang, X. Song, C. Liu, J. He, W. H. Chong and H. Chen, *ACS Nano*, 2014, **8**, 8063-8073.
56. H. Xia, G. Su and D. Wang, *Angew. Chem. Int. Ed.*, 2013, **52**, 3726-3730.

## Table of Content



The two-step pH-programmable self-assembly generates sophisticated "multi-block" chains.